IMPROVING THE CONTROL AND RELIABILITY OF AN ELECTRO-MECHANICAL ACTUATOR

R. Dixon[1] and A.W. Pike[2]

[1]*Electronic & Electrical Engineering Dept, Loughborough University, LE11 3TU, UK.*
[2]*ALSTOM Power Technology Centre, Whetstone, LE8 6LH, UK*
Email: r.dixon@lboro.ac.uk

Abstract: By combining the disciplines of control design, condition monitoring and fault detection identification and accommodation, it should be possible to provide actuators that possess: consistent and tuneable closed-loop performance, a tolerance to sensor faults and the ability to detect actuator deterioration early. This will lead to improved reliability and availability of the actuator. This paper discusses research carried-out to enable the inclusion of advanced control design, fault detection and condition monitoring schemes in an electro-mechanical actuator. The results in the paper were obtained on a laboratory scale actuator in test laboratories at the ALSTOM Power Technology Centre, Whetstone, UK.

Keywords: model-based control, monitoring, fault detection, parameter estimation

1. INTRODUCTION

This paper discusses research carried-out at ALSTOM's test labs to demonstrate the feasibility of including advanced control design, fault detection and condition monitoring schemes in an electro-mechanical actuator (see Fig. 1). The research that is described and the development of the lab-scale system was carried out as part of a larger programme, "REACTS" (see *Dixon et al*., 1999). The target application for REACTS was an aerospace actuator, operating in a harsh environment and with a relatively low duty cycle and with restricted access (for maintenance purposes).

There have been a wide variety of papers concerning topics such as true-digital-control design, fault detection identification and accommodation (FDIA) and condition monitoring. Good introductions to the respective topics can be obtained by reading, for example, (Taylor et al 2000), (Patton, 1997) and Isermann and Balle, 1996). It is clear that these three disciplines should be capable of being combined to provide consistent and tuneable closed-loop performance, tolerance to sensor faults, and early detection of actuator deterioration. In short: improved reliability and availability. For this study, the algorithmic components of the drive system (the control, FDIA and condition monitoring) are each designed independently, but based on a common model of the system. The three elements are implemented on the lab-scale actuator and tested.

The paper is set out as follows: the laboratory scale actuator is described followed by a description of the actuator's dynamic model. This is followed by sections on control design, fault detection and condition monitoring. In each of these sections, results are presented that were obtained from the laboratory scale actuator. The paper concludes with a brief discussion and identifies future work.

2. LAB-SCALE SYSTEM

The lab-scale actuator consists of a brushless DC motor driving into a ballscrew via a gearbox as shown in Fig. 1. The key system sensors for loop closure are current, speed and position, though there are others that are part of the experimental set-up. The actuator is connected via ADC/DAC cards to a dSPACE processor (DSP) that is combined with MATLAB/SIMULINK to provide an environment for algorithm design, rapid prototyping and test.

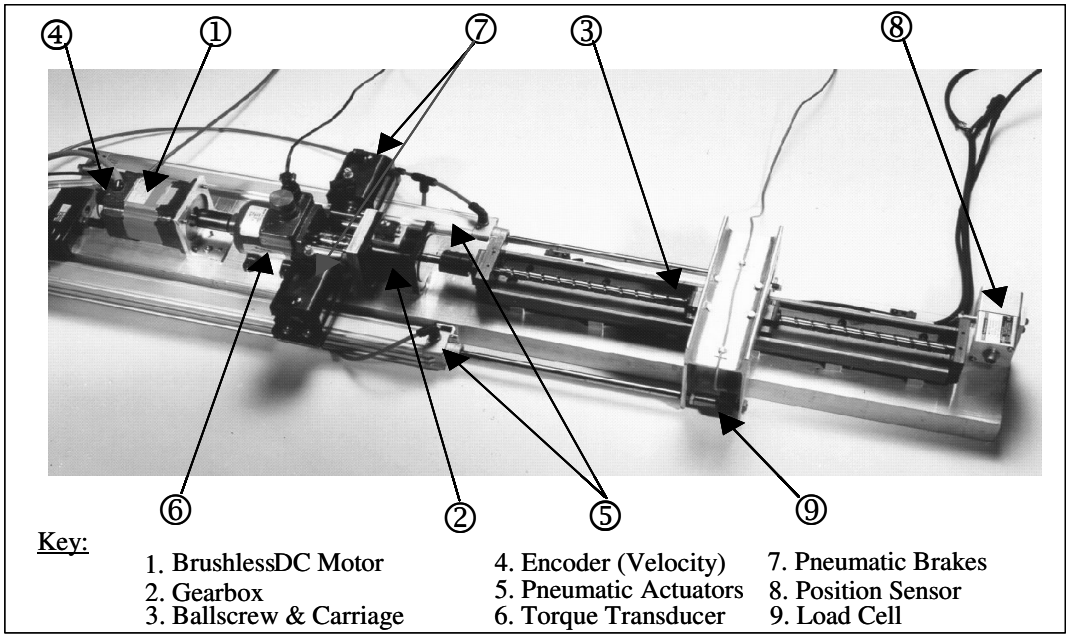

Fig. 1: The laboratory scale actuator - showing the key components of the test system

3. MODELLING THE SYSTEM

A linear model is required as the starting point for the designs that will be considered later. The model can be developed, as shown by the SIMULINK diagram in Fig. 2, using graphical methods and by making use of the physical electrical and mechanical equations of a dc motor. Of course minor extensions are required to represent the amplifier (a linear gain) and the gearbox and ballscrew (linear gains), to provide ballscrew position. Simplifying assumptions in the model include: perfect commutation, only viscous friction acts on the system, and no external load is applied.

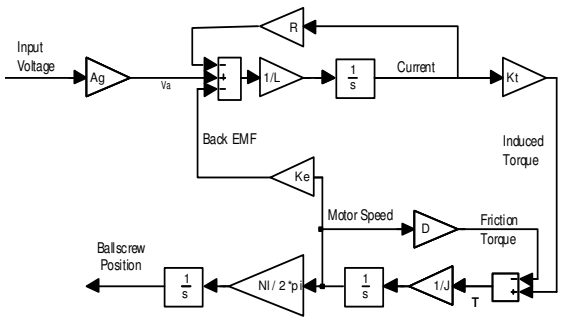

Fig. 2: Linear model of amplifier, brushless DC motor, gearbox, and ballscrew (note: the symbols are defined below).

Inspection of the model diagram (Fig. 2) reveals that there are 3 states (the integrators) and, indeed, it is straightforward to re-write the equations of the system in state-space form.

The state space model takes the usual form:

$$\dot{\mathbf{x}} = \mathbf{A}\mathbf{x} + \mathbf{B}u$$
$$\mathbf{y} = \mathbf{C}\mathbf{x} \qquad (1)$$

where the state vector is, $\mathbf{x} = [I \quad \omega \quad x]^T$,and I, ω and x represent the motor current, motor shaft speed and ballscrew position, respectively. The input u is the voltage applied to the amplifier input and the state transition, input and observation matrices for the model are:

$$\mathbf{A} = \begin{bmatrix} -R/L & -K_e/L & 0 \\ K_t/J & -D/J & 0 \\ 0 & N.l/2.pi & 0 \end{bmatrix}; \ \mathbf{B} = \begin{bmatrix} A_g \\ 0 \\ 0 \end{bmatrix}; \ \mathbf{C} = \begin{bmatrix} 1 & 0 & 0 \\ 0 & 1 & 0 \\ 0 & 0 & 1 \end{bmatrix} \qquad (2)$$

In the above, J is the system inertia (referred to the motor shaft), D is the system's viscous friction (referred to the motor shaft), K_e is the motor back-emf constant, K_t is the motor torque constant, L is the motor winding inductance, R is the winding resistance, N is the gearbox ratio, l is the ballscrew lead and A_g is the amplifier gain. Note that D and J include terms corresponding to the properties of the gearbox and ballscrew.

4. CONTROLLER DESIGN

A typical controller for a motor driven positioning system consists of three cascaded PI (Proportional + Integral) loops acting in turn on current, velocity and position. Often the current loop is implemented in analogue form within the drive amplifier and the gains are fixed by the values of resistors, capacitors etc. The control engineer can then carry out the tuning of the two outer-loops, in order to ensure a particular overall closed-loop performance. Selection of appropriate values for the four gains (two proportional, two integral) can be a lengthy process and the final performance may well be less than optimal in some sense. Even though the exact desired performance may be physically possible, the engineer may be unable to realise it due to time or other constraints.

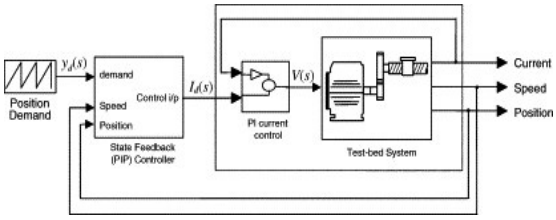

Fig. 3. Proportional-Integral-Plus position control scheme for the test-bed.

Fig. 3 shows an alternative controller structure that consists of proportional and integral gains on position and a proportional velocity gain. This implementation is sometimes known as Proportional-Integral-Plus (PIP) control, which can be designed within a True Digital Control (TDC) framework as introduced by Young *et al* (1987). It shares many of the excellent properties of the well known PI or PID controllers, but also exploits the additional power of State-Variable-Feedback (SVF) design techniques. In the present case, the directly measurable states are the sampled values of the position, velocity and the integral of the position error.

Adoption of the TDC approach means that the entire control design is undertaken in discrete time. The design process includes: identification and estimation of a discrete time data-based model followed by design of the PIP control algorithm using this model. Its application to the test-bed is summarised below.

4.1 System Identification and Parameter Estimation

Identification: It is not necessary to identify the model structure via experiment as it is known, via physical modelling, from (1) and (2). There is a slight complication in that a current control PI loop is already in place. However, as the nature of this is also known the model can be augmented to include the current control and then, as the current response is designed to be much faster than the rest of the system, the states corresponding to the current controller can be removed. In physical terms this is equivalent to assuming that the current applied to the motor is always the same as that demanded by the position control system.

Following the above procedure yields a system with two states (speed and position) that can be transformed to discrete time (using for example a zero order hold), so that the structure of the model is known apriori. That is:

$$\begin{bmatrix} \omega(k) \\ x(k) \end{bmatrix} = \begin{bmatrix} a_{11} & a_{12} \\ a_{21} & a_{22} \end{bmatrix} \begin{bmatrix} \omega(k-1) \\ x(k-1) \end{bmatrix} + \begin{bmatrix} b_1 \\ b_2 \end{bmatrix} I(k-1) \qquad (3)$$

where $I(k)$, $\omega(k)$ and $x(k)$ represent the motor current, motor shaft speed and ballscrew position at sample k respectively. The parameters requiring estimation in (3) are a_{11}, a_{12} and b_1. The other parameters (a_{21}, a_{22} and b_2) are calculated directly from the *known* gear ratio and ballscrew lead because, unlike the former parameters, these are not expected to change as the rig ages.

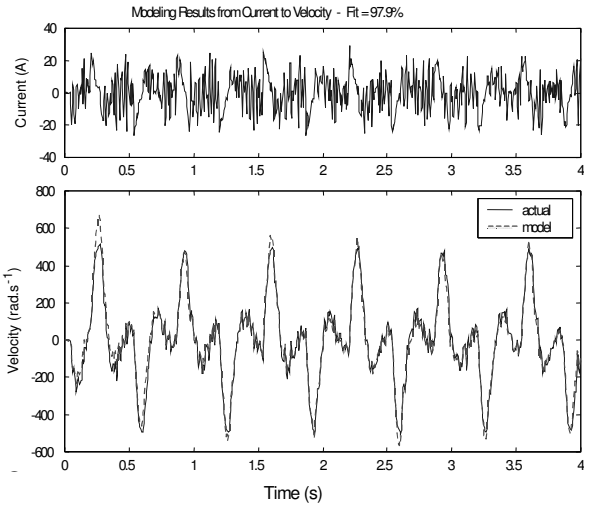

Fig. 4. Control modelling results showing the input (current) to the system, the system output (velocity) and the model output.

Estimation: This involves first collecting data from a carefully designed experiment. In this case the experiment is carried-out in closed loop following a repeating sequence of step inputs and with band-limited white noise injected directly onto the current demand. Following data collection, the parameters of the discrete-time model are estimated by fitting the model to the data using the Simplified Refined Instrumental Variable (SRIV) method (Young, 1985). The ensuing TF model is then transformed to state space form and extended to include the known physical properties of the gearbox and ballscrew (parameters a_{21}, a_{22} and b_2). A typical set of modelling results can be seen in Fig. 4, above.

Evaluation of the model is carried-out by visual inspection and by statistical measures such as the Coefficient of Determination, R_T^2.

$$R_T^2 = 1 - \frac{\sigma^2}{\sigma_y^2} \qquad (4)$$

where σ^2 is the sampled variance of the model residuals (or model error) and σ_y^2 is the sample variance of the measured system output about its mean value. This 'goodness of fit' criterion tends to unity as the fit of the model to the data improves. In this work the model fit is described as a percentage (i.e, $R_T^2 \times 100\%$) and the model fit for the results in Fig. 4 is 98%

4.2 PIP Control Law Design

Design of the PIP controller involves first augmenting the state-space model (3) with an integral-of-position-error state and then designing a SVF control law. The control law associated with the augmented model takes the usual SVF form,

$$u(k) = -\mathbf{k}\mathbf{x}(k) \qquad (5)$$

The gain vector, **k**, is selected using pole placement as described below.

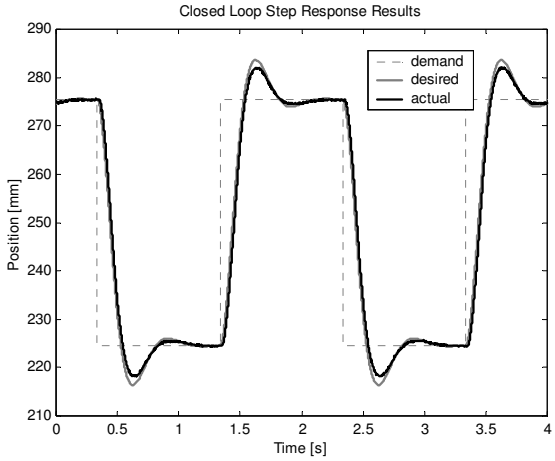

Fig. 5. Closed-loop response of system with desired natural frequency of 2Hz and damping of 0.5.

The desired closed-loop response is specified by choice of a (second order) natural frequency and damping ratio. The first two closed-loop poles are then placed to achieve this and the third is set to be around 10 times faster (thereby having little effect). The PIP controller itself is then implemented in an incremental form (to avoid integrator wind-up) on the dSPACE hardware. A set of results for the closed loop response compared with that desired is shown in Fig. 5.

Using the model-based approach described above for calculating control gains, yields a controller that can be rapidly re-tuned, either to accommodate changes in the system or to modify the closed-loop performance.

5. FAULT DETECTION IDENTIFICATION & ACCOMMODATION

It is recognised that there are many ways of tackling the problem of FDIA, many of which are discussed by Patton, (1997). However, the inspiration for the work described here came from suggestions made by Clark *et al.* (1975). Whilst the approach appears to be relatively simple, it is found to yield reasonable results. For the detailed design see (Dixon, 2004), the approach and results are summarised below.

Three linear observers (or Kalman filters) are used to detect and identify faults corresponding to the system's three sensors. The observers are based on the model described by equations (1) and (2) and are designed together with their associated detection algorithms to be insensitive to model errors and unmeasured disturbances whilst remaining sensitive to faults on their respective sensor. Having successfully detected a sensor fault, a reconstructed measure of the corresponding output signal (generated from an observer not associated with the faulty sensor) is used to replace the measured signal for feedback control. This ensures that the system remains stable and continues to function effectively even after a sensor failure. Up to two simultaneous faults can be accommodated. The algorithms were implemented in dSPACE and a number of tests were carried-out, three of which are discussed below:

5.1 Velocity fault

Fault accommodation disabled: The first stage of this experiment demonstrates the system behaviour with a loss of velocity measurement and no FDIA present. The position response can be seen in Fig. 6. Between 2.8 and 6.8 seconds, when loss of velocity measurement occurs, the position of the actuator becomes highly oscillatory. During this period, the velocity fault flag indicates a fault to be present but the accommodation is disabled.

Fault accommodation enabled: The second part of the experiment is similar to the first test. However, this time the FDIA is enabled and Fig. 7 shows the effectiveness of the FDIA scheme in detecting the velocity sensor fault and accommodating the fault by providing an analytical velocity signal to the controller. As a consequence the closed-loop performance remains acceptable and there is no oscillatory behaviour. If required, the system could continue to operate in this state indefinitely. Note that on reconnection of the sensor (7.4 seconds) the detection algorithm recognises correct operation and toggles the fault flag to the false state, allowing the measured velocity feedback to be resumed.

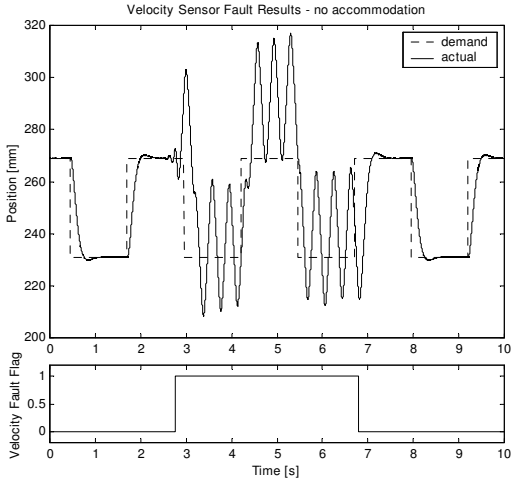

Fig. 6. Velocity fault results – FDIA disabled

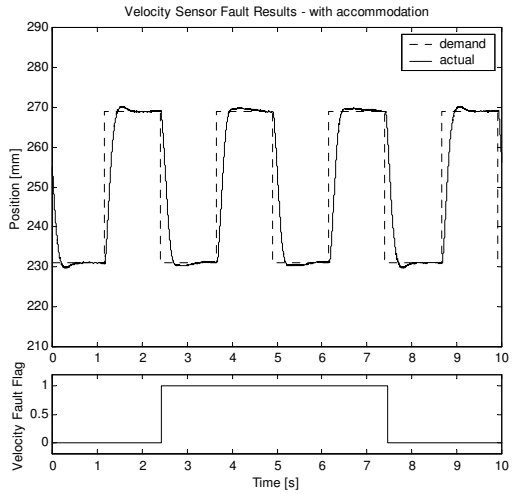

Fig. 7. Velocity fault results – FDIA enabled

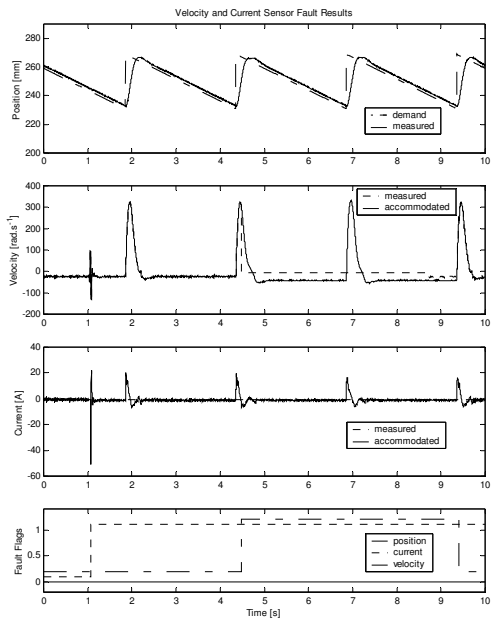

Fig 8 Current and Velocity fault results

5.2 Current and Velocity faults

If unaccommodated, these faults would lead to unacceptable (perhaps even catastrophic) behaviour of the system. However, it can be seen from Fig. 8 that a current sensor failure followed by a failure of the velocity sensor can be both detected and accommodated to allow the system to continue operating with minimal loss of performance. At approximately 1 second the current fault occurs and is detected and accommodated. When the second fault occurs at 4.5 seconds, this too is detected and accommodated in a timely fashion. In this case, Fig. 8 illustrates the position output and fault flags (top and bottom plots respectively) together with both accommodated and measured values for the velocity and current signals (middle two plots). Note that, for clarity, the fault flags are offset from each other.

6. CONDITION MONITORING

Here discrete time parameter estimation is combined with the physical model of the system to facilitate the estimation of non-measurable physical process parameters from measured signals. The result is a short 2 to 4 second test that provides estimates of the six key physical parameters (resistance, inductance, friction, inertia, torque constant and back-emf constant) of the electromechanical positioning system. In brief, the parameters are calculated via a transfer function model of the system, which is obtained from time history data using SRIV (Young 1985). The estimates are then assessed against base-line parameters and trended historically for monitoring purposes. Ultimately, the control system can use the estimates to provide an early warning of incipient faults, rather than simply reporting a failure after the event.

Estimation of the physical system parameters relies on the following five step procedure:

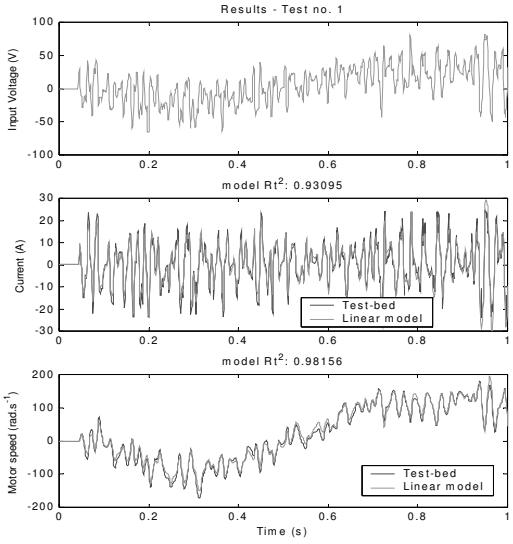

Fig. 9. Parameter estimation results for test 1 of friction experiment (i.e., no change)

1) Perturbation of the system with a suitable input signal (*band-limited white noise*) and recording of the resulting input-output data
2) Estimation using SRIV of the parameters of a suitably identified discrete time linear model of the system.
3) Model assessment (using $R_T^2 \times 100\%$) to ensure it is sufficiently accurate.
4) Transformation of the discrete model to a continuous time model.
5) Algebraic transformation of the continuous time model parameters to the key physical parameters of the system.

The detailed technical steps in this procedure are discussed in (Dixon and Pike, 2002) alongside several sets of validation results. Two such experiments are presented below.

6.1 Increasing Friction

Seven tests of 4 seconds duration were conducted on the actuator. In the first test there is no change in the friction, for the remaining six the friction is increased incrementally (in a linear fashion) by application of the brake. Fig. 9 shows a one second section of data collected and the model fitting results for test 1 (i.e., fault free case). As can be seen the dominant modes are captured by the model, with individual model fits of 93.1% and 98.2% indicating an overall fidelity of 95.7%.

The results presented in Fig. 10 show the algorithm output based on the seven tests. Each subplot shows the percentage change of a particular parameter when compared to its nominal value.

It can be seen that the estimation algorithm is correctly picking-up the change in friction. There is also some degree of cross-coupling with the other parameters (which do not change in practice), though this is at least an order-of-magnitude less than the friction change. It is clear from inspection that the developing problem is friction related.

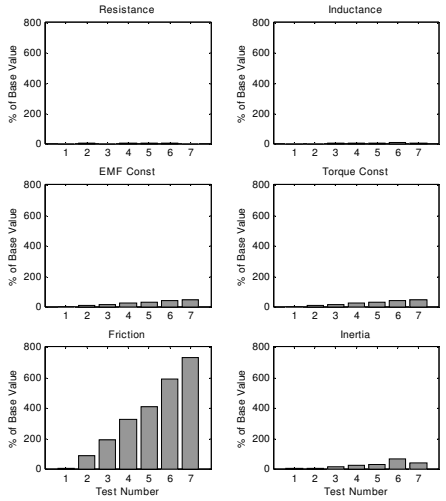

Fig. 10. Estimated parameter change over seven tests with increasing Coulomb friction (D).

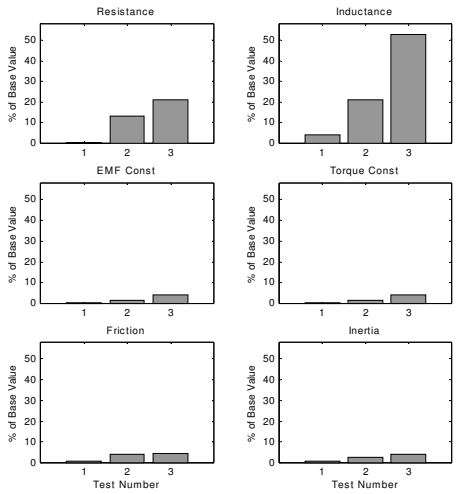

Fig. 11 Estimated parameter change over three tests with increasing inductance (*L*) and resistance (*R*).

6.2 Increased Inductance and Resistance

For this experiment, hand-wound inductors were placed in series with the phase windings of the motor. The inductors were designed to generate inductance changes of 0.25mH and 0.6mH, i.e., 20% and 50% respectively on top of the manufacturers quoted values (Note that the inductance values have some variability with current due to saturation effects and other core non-linearities). The measured additional resistances due to the wire where 0.13Ω and 0.2Ω respectively (or about 13% and 20%).

7. CONCLUSIONS

The paper has given an overview of research work carried out to combine the benefits of model based control, monitoring and fault detection and accommodation on a laboratory scale actuator. The set of implementation results presented illustrate the potential usefulness of such an approach for improving actuator reliability and availability. The techniques and algorithms employed are generic and should be readily extensible to other types and configurations of actuator.

Whilst the results obtained are promising, the three systems (control, FDIA and monitoring) were developed in a slightly ad-hoc fashion and independently of one-another. This is considered to be a potential weakness: for example, interaction between the various algorithms may occasionally produce a deleterious effect on the overall system performance. Future work at Loughborough (with collaboration from ALSTOM) aims to develop a more rigorous framework for the integrated design of such systems.

ACKNOWLEDGEMENTS

The authors would like to thank the ALSTOM POWER Technology Centre for permission to publish this paper. The work was part funded by the UK DTI under the CARAD initiative.

REFERENCES

Isermann, R. and P. Balle (1996) Trends in the application of model based fault detection and diagnosis of technical processes, *Proc. of IFAC 13th World Congress, San Francisco, USA*, pp 1-12.

Dixon, R. (2004) Observer-based FDIA: application to an electromechanical positioning system, *Control Engineering Practice*, **Vol. 12**, Issue 9, Pages 1113-1125.

Dixon, R. and A.W. Pike, (2002), Application of condition monitoring to an electro-mechanical actuator: a parameter estimation based approach, *Computing & Control Engineering Journal*, IEE, **Vol. 13,** No. 2, pp. 71-81.

Dixon, R, N. Gifford, C. Sewell & M.C. Spalton, (1999). REACTS: Reliable Electrical Actuation Systems, *Proc. of IEE Colloquium on Electrical Machines & Systems for the More Electric Aircraft*, IEE ref. 99/180 London, Nov. 1999.

Patton, R.J. (1997) Fault-Tolerant Control: The 1997 Situation, Proc. of 3rd Symposium on Fault detection, supervision and safety for technical processes,Hull, UK, **Vol.3** pp.1029-1052.

Taylor, C.J., Chotai, A. and Young, P.C., (2000), State space control system design based on non-minimal state-variable feedback : Further generalisation and unification results, *Int. J. of Control*, **73**, pp.1329-1345.

Young, P.C. (1985) The instrumental variable method: A practical approach to identification and system parameter estimation, appears in H.A. Barker and P.C. Young (Eds.), *Identification and System Parameter Estimation,* Pergamon, Oxford, pp. 1-15.

Young, P.C., M.A. Behzadi, C.L. Wang and A. Chotai (1987) Direct digital and adaptive control by input-output, state variable feedback pole assignment. *Int. J. of Control*, **46**, pp. 1867-1881.

Clark, R.N., Fosth D.C., & Walton W.M. (1975) Detecting instrument malfunctions in control systems. *IEEE Transactions on Aerospace and Electronic Systems*, **16**, pp.468-473